Whole-Exome Sequencing Defines the Mutational Landscape of Pheochromocytoma and Identifies *KMT2D* as a Recurrently Mutated Gene

C. Christofer Juhlin,[1,2,3]* Adam Stenman,[3] Felix Haglund,[3] Victoria E. Clark,[4] Taylor C. Brown,[1,2] Jacob Baranoski,[4] Kaya Bilguvar,[5] Gerald Goh,[6,7] Jenny Welander,[8] Fredrika Svahn,[3] Jill C. Rubinstein,[1,2] Stefano Caramuta,[3] Katsuhito Yasuno,[4,6] Murat Günel,[4] Martin Bäckdahl,[9] Oliver Gimm,[8,10] Peter Söderkvist,[8] Manju L. Prasad,[11] Reju Korah,[1,2] Richard P. Lifton,[6,7,12] and Tobias Carling[1,2]*

[1]Yale Endocrine Neoplasia Laboratory, Yale School of Medicine, New Haven, CT 06520
[2]Department of Surgery, Yale School of Medicine, New Haven, CT
[3]Department of Oncology-Pathology, Karolinska Institutet, Karolinska University Hospital, CCK, Stockholm, Sweden
[4]Department of Neurosurgery, Yale Program in BrainTumor Research, Yale School of Medicine, New Haven, CT
[5]Department of Genetics and Yale Center for Genome Analysis, Yale School of Medicine, New Haven, CT
[6]Department of Genetics, Yale School of Medicine, New Haven, CT
[7]Howard Hughes Medical Institute, Yale School of Medicine, New Haven, CT
[8]Department of Clinical and Experimental Medicine, Faculty of Health Sciences, Linköping University, Linköping SE-58185, Sweden
[9]Department of Molecular Medicine and Surgery, Karolinska Institutet, Karolinska University Hospital, Stockholm, Sweden
[10]Department of Surgery, County Council of Östergötland, Linköping SE-58185, Sweden
[11]Department of Pathology, Yale School of Medicine, New Haven, CT
[12]Yale Center for Mendelian Genomics, New Haven, CT

As subsets of pheochromocytomas (PCCs) lack a defined molecular etiology, we sought to characterize the mutational landscape of PCCs to identify novel gene candidates involved in disease development. A discovery cohort of 15 PCCs wild type for mutations in PCC susceptibility genes underwent whole-exome sequencing, and an additional 83 PCCs served as a verification cohort for targeted sequencing of candidate mutations. A low rate of nonsilent single nucleotide variants (SNVs) was detected (6.1/sample). Somatic *HRAS* and *EPAS1* mutations were observed in one case each, whereas the remaining 13 cases did not exhibit variants in established PCC genes. SNVs aggregated in apoptosis-related pathways, and mutations in COSMIC genes not previously reported in PCCs included *ZAN*, *MITF*, *WDTC1*, and *CAMTA1*. Two somatic mutations and one constitutional variant in the well-established cancer gene *lysine (K)-specific methyltransferase 2D* (*KMT2D*, *MLL2*) were discovered in one sample each, prompting *KMT2D* screening using focused exome-sequencing in the verification cohort. An additional 11 PCCs displayed *KMT2D* variants, of which two were recurrent. In total, missense *KMT2D* variants were found in 14 (11 somatic, two constitutional, one undetermined) of 99 PCCs (14%). Five cases displayed somatic mutations in the functional FYR/SET domains of KMT2D, constituting 36% of all *KMT2D*-mutated PCCs. *KMT2D* expression was upregulated in PCCs compared to normal adrenals, and *KMT2D* overexpression positively affected cell migration in a PCC cell line. We conclude that *KMT2D* represents a recurrently mutated gene with potential implication for PCC development.

Additional Supporting Information may be found in the online version of this article.

**Correspondence to*: C. Christofer Juhlin, Karolinska University Hospital, CCK R8:04, Stockholm, SE-17176, Sweden. E-mail: christofer.juhlin@ki.se or Tobias Carling, Yale School of Medicine, 333 Cedar Street, FMB130A, Box 208062, New Haven, CT 06520. E-mail: tobias.carling@yale.edu

Supported by: The Stockholm County Council (clinical postdoctoral appointment; CCJ); StratCan, Karolinska Institutet, Stockholm (AS); The Agency for Science, Technology and Research, Singapore (GG); The Cancer Society in Stockholm, Sweden (MB); RPL is an Investigator of the Howard Hughes Medical Institute; The Damon Runyon Cancer Research Foundation (TC is a Damon Runyon Cancer Research Foundation clinical investigator); An Ohse Research Award.

Received 18 March 2015; Revised 8 May 2015; Accepted 10 May 2015

DOI 10.1002/gcc.22267

Published online 29 May 2015 in
Wiley Online Library (wileyonlinelibrary.com).

INTRODUCTION

Pheochromocytomas (PCCs) are rare, predominantly benign tumors arising from chromaffin cells of the adrenal medulla. Patients with PCC are diagnosed using catecholamine screening along with cross-sectional imaging and treated surgically (Welander et al., 2011; Brito et al., 2015). Approximately 40% of patients with PCCs have been reported to carry germline mutations in a growing list of genes (Dahia, 2014) currently including *FH*, *EGLN1*, *EPAS1*, *KIF1Bβ*, *MAX*, *NF1*, *RET*, *SDHA*, *SDHB*, *SDHC*, *SDHD*, *SDHAF2*, *TMEM127*, and *VHL* (Crossey et al., 1994; Ladroue et al., 2008; Schlisio et al., 2008; Qin et al., 2010; Comino-Méndez et al., 2011; Welander et al., 2011; Zhuang et al., 2012; Castro-Vega et al., 2014; Dahia, 2014; Brito et al., 2015). Germline mutations in several of these susceptibility genes cause adrenomedullary tumor syndromes in which the patient presents with PCCs in addition to various syndromic manifestations (Favier et al., 2015), *NF1* mutations cause neurofibromatosis type 1 in which 5% of patients can develop PCCs, *RET* mutations cause multiple endocrine neoplasia type 2, *VHL* mutations cause the von Hippel–Lindau syndrome, mutations in diverse *SDHx* genes have been linked to different hereditary paraganglioma and/or PCC syndromes named PGL1-4, mutations in *EPAS1*/*HIF2A* have been associated with the polycythemia-paraganglioma syndrome (Zhuang et al., 2012) and the Reed syndrome gene *FH* was recently found mutated in PCCs (Castro-Vega et al., 2014). Gene expression analyses have revealed that the PCCs can be clustered into mainly two different subgroups relating to genetic events and their aberrant pathways: *VHL*/*SDHx*/*EPAS1*-mutated tumors associate to stabilization of hypoxia inducible factors while *KIF1Bβ*/*MAX*/*NF1*/*RET*/*TMEM127*-mutated tumors correlate to the activation of kinase signalling pathways (Eisenhofer et al., 2004; Schlisio et al., 2008; Dahia, 2014; Welander et al., 2014a; Favier et al., 2015). The genetics underlying sporadic PCCs are not yet clearly understood, and a majority of the tumors still lack a defined genetic driver event (Welander et al., 2011; Favier et al., 2015). Even so, somatic inactivating *neurofibromin 1* (*NF1*) tumor suppressor gene mutations was recently discovered as a frequent event in PCCs (Burnichon et al., 2012; Welander et al., 2012) in addition to activating *HRAS* and *EPAS1* mutations in subsets of cases (Comino-Méndez et al., 2013; Crona et al., 2013).

To further characterize the mutational landscape of adrenomedullary tumors and to identify novel gene candidates involved in disease development, 15 PCCs lacking established PCC susceptibility gene mutations as well as one *RET*-mutated PCC were collected and subjected to whole-exome sequencing (WES), and candidate genes were validated in an expanded cohort.

MATERIALS AND METHODS

Sample Acquisition, Preparations, and Ethical Statements

The study comprised a total of 99 PCCs; 89 Swedish cases and 10 US cases (Supporting Information Table 1). The PCCs are divided into a discovery cohort of 16 cases and a verification cohort of 83 cases. The discovery cohort subjected to WES consisted of fresh-frozen samples from 16 matched pairs of histologically confirmed PCC and normal tissues collected from surgery specimen at the Karolinska University Hospital, Stockholm, Sweden, and the verification cohort consisted of fresh-frozen tissues from a total of 83 histologically confirmed PCCs; 73 samples from the Karolinska University Hospital and 10 samples from the Yale-New Haven Hospital, New Haven, CT. All cases have been histologically confirmed as PCCs using World Health Organization (WHO) criteria as part of the routine histopathology work-up (DeLellis et al., 2004). The distinction between malignant and benign PCCs was evaluated using the Armed Forces Institute of Pathology criteria (AFIP; Lack, 2007). All discovery cohort cases ($n = 16$) as well as approximately 70% of the cases in the verification cohort collected for extraction of genomic DNA were of sufficient sizes to allow for recutting and review by an experienced pathologist to confirm the representativity of PCC and eventual matched normal tissue for each case in parallel to the DNA extraction process (data not shown). Genomic DNA from somatic and constitutional tissues was extracted and validated using the DNeasy Blood and Tissue DNA isolation kit (Qiagen, Hilden, Germany) and Nano-Drop technology. DNA was obtained from both tumor and constitutional tissues for all cases in the discovery cohort and subsequently subjugated to WES. As the exome sequencing was carried out in parallel for tumor and matched constitutional DNA for each case, recurrently mutated candidate genes on the somatic level were subsequently checked for germline variants using the exome sequencing data retrieved from constitutional tissues. The attaining of tissue and subsequent genomic analyses from both institutions were permitted by the local ethical

review board at Karolinska Institutet, Stockholm, Sweden and the Yale University Institutional Review Board, New Haven, CT, respectively.

Clinical and Genetic Characteristics

The overall clinical and genetic characteristics of the discovery and verification cohorts are detailed in Supporting Information Table 1. The discovery cohort of 16 PCCs used for WES includes 15 tumors (11 benign and 4 malignant PCCs) previously screened and found wild type for mutations in 13 known PCC susceptibility genes, namely *EGLN1*, *KIF1Bβ*, *MAX*, *MEN1*, *NF1*, *RET*, *SDHA*, *SDHB*, *SDHC*, *SDHD*, *SDHAF2*, *TMEM127*, and *VHL* (Welander et al., 2014b). A PCC from a MEN2 patient exhibiting a constitutional *RET* gene mutation was also added to the discovery cohort, as this case displayed a highly equivocal pathology report suggestive of malignant features, but not fulfilling the AFIP or the WHO criteria for malignancy. As a very low PCC malignancy rate is reported for MEN2a patients, we analyzed this case as a part of the discovery cohort to pinpoint additional somatic driver mutations which could bear significance for malignant transformation in MEN2 PCCs. At the time of submission of the PCC discovery cohort for WES, the *EPAS1* mutational status of the 16 cases was not known. Approximately 6 months after the submission of the discovery cohort material for WES, *EPAS1* gene mutational status was included in the original study (Welander et al., 2014b).

Mutational data were available for 73 of the 83 PCCs included in the verification cohort, and the information was collected from three independent studies (genes investigated within parenthesis); (Welander et al., 2014a) (*EPAS1*, *TMEM127*), (Welander et al., 2012) (*MAX*, *NF1*, *SDHB/D*, *RET*, *VHL*) and (Welander et al., 2014b) (*EGLN1*, *EPAS1*, *KIF1Bβ*, *MAX*, *MEN1*, *NF1*, *RET*, *SDHA/B/C/D*, *SDHAF2*, *TMEM127* and *VHL)*. These data are detailed in Supporting Information Table 1.

Exome Capture, Massively Parallel Sequencing, Analysis, and Expressional Studies

Genomic DNA samples generating adequate high-quality libraries were subjected to exome capture and sequencing, and the complete methodology regarding WES, sequence validation, ontology analyses, statistics, expressional analyses, and functional experiments are detailed in the Supporting Information Materials and Methods.

RESULTS

WES of the Discovery Cohort

Using WES, a total of 130 somatic single nucleotide variants (SNVs) were detected across the 16 samples in the discovery cohort, with an individual tumor SNV count ranging from 0 to 18. Of the 130 SNVs detected, 97 (75%) were nonsynonymous, on average 6.1/sample (Fig. 1A, Supporting Information Table 2). Eighty-eight were missense alterations, five were positioned at exon–intron boundaries, and four were nonsense (truncating mutations). A mean coverage of 217 and 103 reads in tumor and normal samples, respectively, was obtained. Tumor samples were intentionally sequenced to a greater depth than normal tissue to maximize detection of heterozygous mutations in tumor cells intermingled with adjacent stromal tissue. Tumor purity ranged from 20.5 to 89.6% with a mean purity of 59%.

Somatic Mutations in PCC-Related Genes

Variants in PCC-related genes included the previously established constitutional *RET* variant in Case 34 as well as somatic mutations in *HRAS* (Q61R) and *EPAS1* (P531S) in one case each (cases 88 and 94, respectively); however, the remaining 13 cases did not display any variant in PCC-associated genes. The *HRAS* Q61R mutation is a well-established activating variant that has been previously demonstrated in PCCs (Crona et al., 2013). The *EPAS1* mutation P531S mutation has been similarly found in adrenomedullary tumors previously, and this variant affects the *EPAS1* prolyl hydroxylation site (residues 530–539), which modulates the oncogenic function of *EPAS1* (Comino-Méndez et al., 2013). While Case 88 lacks other somatic mutations in cancer-related genes, Case 94 also displays a heterozygous missense variant in the *TSC2* tumor suppressor gene (Fig. 1A).

Recurrently Mutated Catalogue of Somatic Mutations in Cancer (COSMIC) Database Genes

KMT2D, also known as *mixed-lineage leukemia 2* (*MLL2*) encoding a histone methyltransferase that regulates DNA accessibility was identified as the most frequently mutated cancer-related gene in our discovery cohort, with two cases exhibiting somatic heterozygous *KMT2D* gene mutations and one additional case harboring a constitutional heterozygous *KMT2D* variant (3/16; 19%) (Fig. 1A, Table 1, Supporting Information Fig. 1). The two somatic mutations (p.N5223S

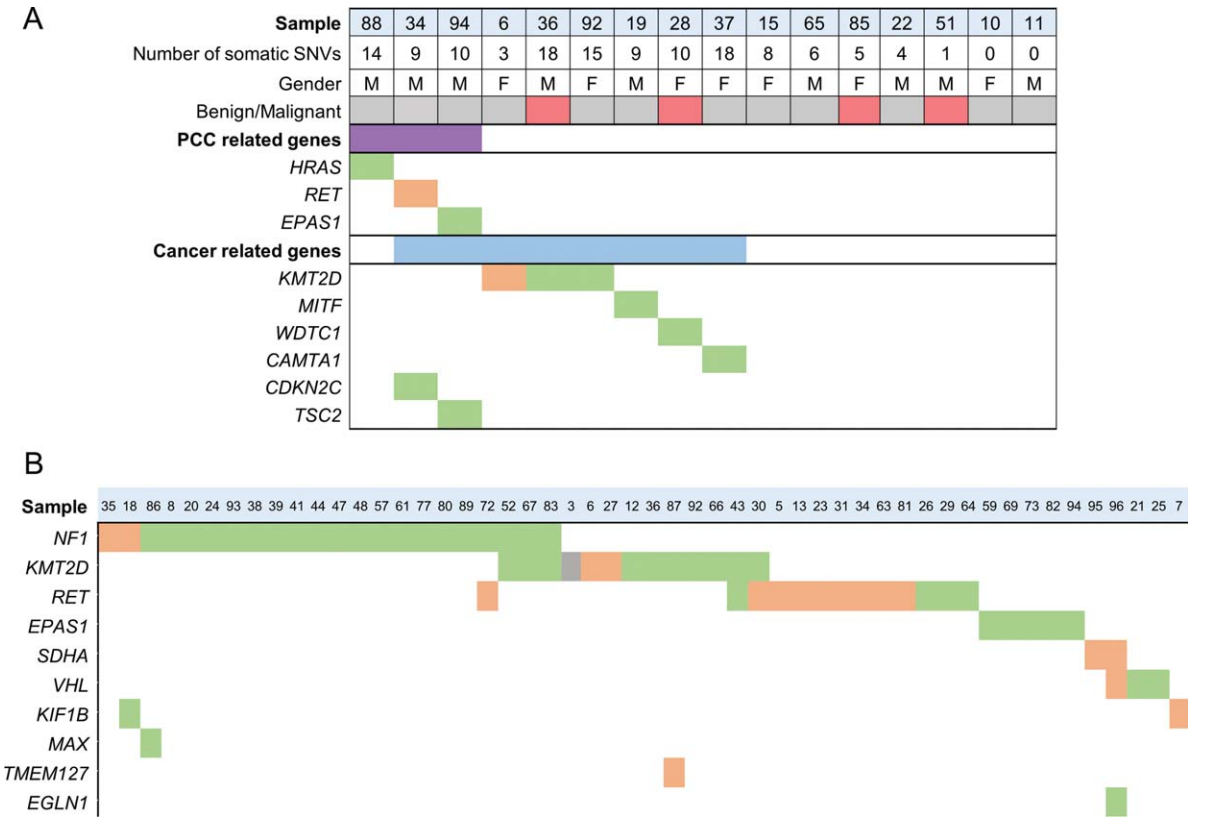

Figure 1. (A) Overall mutational profile of the 16 PCCs included in the whole-exome sequencing discovery cohort. All panels are aligned with vertical tracks representing 16 individuals with PCC, and the underlying heatmap illustrates the distribution of somatic coding mutations in PCC related genes (i.e., genes previously found mutated in PCCs) as well as in cancer-related genes (i.e., COSMIC genes recurrently mutated in several human neoplasias). M: male, F: female. Square color scheme: purple (PCC-related genes), blue (cancer-related genes), gray (benign), red (malignant according to the AFIP criteria), green (somatic mutation), and orange (constitutional variant). (B) Mutational heatmap of all PCCs ($n = 52$) from the discovery and verification cohorts with a previously published variant in a PCC susceptibility gene, including the novel data regarding *KMT2D* variants as comparison. Square color scheme denote mutational category: green (somatic mutation), orange (constitutional variant), and gray (not determined). [Color figure can be viewed in the online issue, which is available at wileyonlinelibrary.com.]

and p.H5420Y) were both allocated to evolutionary conserved amino acid positions within domains of the KMT2D protein with potential conserved roles related to chromatin regulation; namely the FYR-N and SET domains, respectively (Table 1, Fig. 2A). The constitutional variant (p.G2735S) is located in a region without known functional annotations, and is not reported as a polymorphism in the 1000 Genomes or Exome Variant Server databases. All three *KMT2D* variants as well as 13 additional variants from 12 genes detected by WES were confirmed using Sanger sequencing, and detailed information regarding these variants and primer sequences are available in Supporting Information Table 3.

Moreover, somatic missense mutations in the *zonadhesin* (*ZAN*) gene were found in two cases (Case 34; p.T823N and Case 88; p.A2396S). *ZAN* encodes a protein that is involved in sperm adhesion to the zona pellucida of the egg, and is represented in the COSMIC database as a recurrently mutated gene in lung adenocarcinoma and endometroid uterine carcinoma.

Somatic Mutations in Nonrecurrent COSMIC Genes

Several nonrecurrent somatic mutations in COSMIC annotated genes not previously associated to PCC development were observed in cases devoid of other known driver gene mutations (Fig. 1A, Supporting Information Table 2). For example, Case 19 (benign PCC) exhibited a missense p.R324S mutation in the *microphthalmia-associated transcription factor* (*MITF*) oncogene, a gene frequently amplified and mutated in melanoma (Cronin et al., 2009). Case 28 (malignant PCC) displayed a truncating p.L294X mutation in the *WD and tetratricopeptide repeats 1* (*WDTC1*) gene, a candidate driver gene in microsatellite-unstable colorectal cancer (Alhopuro et al., 2012), and Case 37 (benign PCC) exhibited a

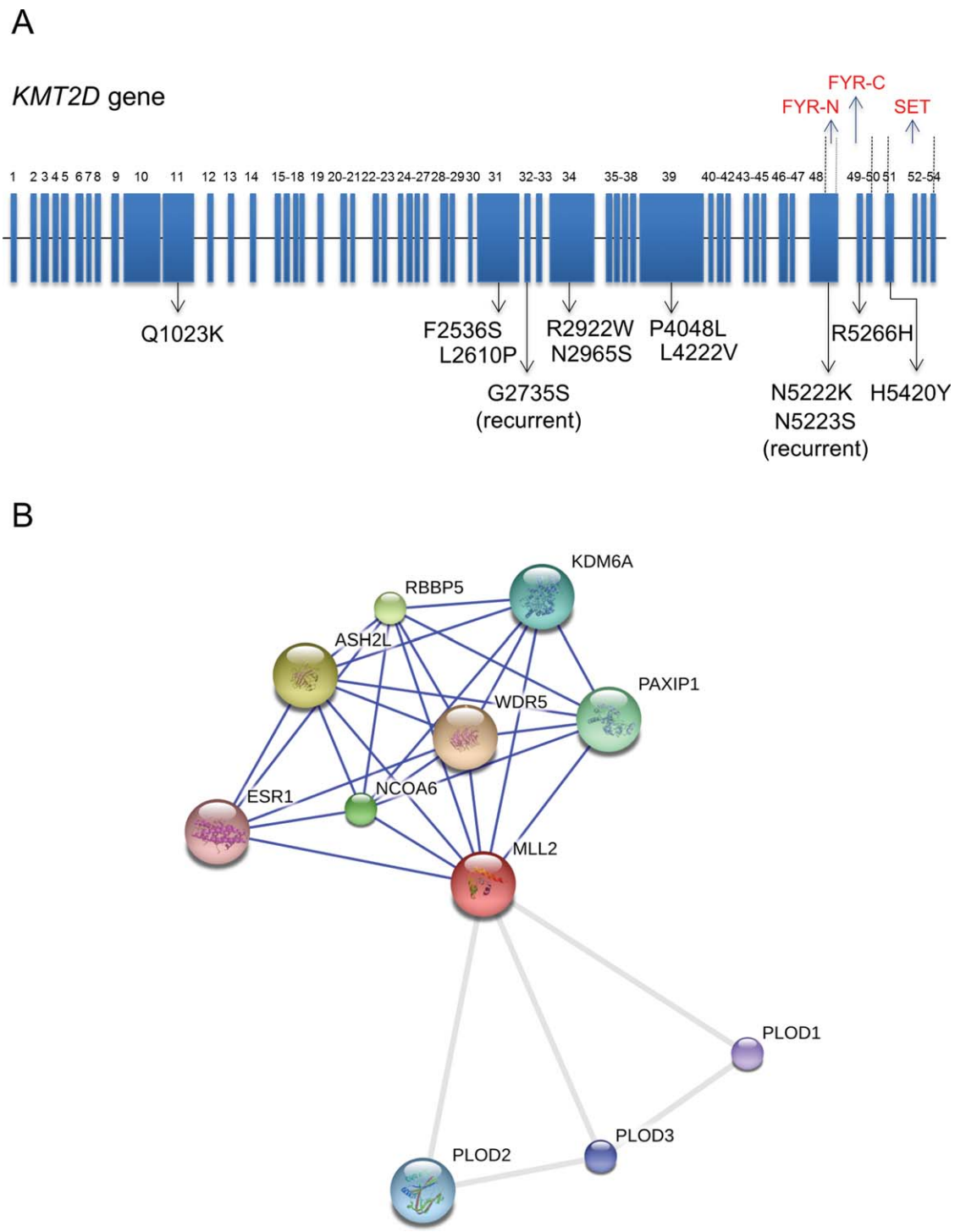

Figure 2. (A) Schematic representation of the *KMT2D* gene and mutational burden in PCCs. The 54 exon-spanning *KMT2D* gene is depicted with arrows indicating exon positions for each of the 14 *KMT2D* missense variants discovered in the discovery and verification cohorts. Recurrent variants (p.G2735S and p.N5223S) were found in two PCC cases each. Mutations within functionally important regions include N5222K/N5223S (FYR-N domain; amino acids 5175-5235), R5266H (FYR-C domain; amino acids 5236-5321), and H5420Y (SET domain; amino acids 5397-5513). (B) Search Tool for the Retrieval of Interacting Genes/Proteins (String) database interaction output illustrating well-characterized KMT2D (MLL2) interacting proteins. Blue lines denote confident binding partners as verified through experimental data and gray lines denote a predicted association in curated databases. [Color figure can be viewed in the online issue, which is available at wileyonlinelibrary.com.]

TABLE 1. Summary and Computational Functional Prediction of the 14 *KMT2D* Gene Variants in 99 Pheochromocytoma Samples

Sample number	Variant (amino acid change)	Nucleotide change	Somatic/ constitutional origin[a]	CHASM driver score[b]	*P* value	CHASM functional score	*P* value	PolyPhen2 score[c]	PolyPhen2 prediction[c]	FYR/SET domain
Discovery cohort (n=16)										
6	G2735S	GGC>AGC	Constitutional	0.562	0.254	0.291	0.318	0.008	Benign	No
36	N5223S	AAT>AGT	Somatic	0.420	0.063	0.174	0.481	0.887	Possibly damaging	FYR-N
92	H5420Y	CAC>TAC	Somatic	0.364	0.030	0.596	0.123	0.998	Probably damaging	SET
Verification cohort (n=83)										
3	G2735S	GGC>AGC	N.d.	0.562	0.254	0.291	0.318	0.008	Benign	No
12	R5266H	CGC>CAC	Somatic	0.504	0.155	0.471	0.184	0.98	Probably damaging	FYR-C
27	Q1023K	CAG>AAG	Constitutional	0.700	0.605	0.119	0.608	0.002	Benign	No
30	N2965S	AAC>AGC	Somatic	0.402	0.052	0.006	0.996	0.000	Benign	No
43	N5223S	AAT>AGT	Somatic	0.420	0.063	0.174	0.481	0.887	Possibly damaging	FYR-N
52	L2610P	CTA>CCA	Somatic	0.394	0.047	0.212	0.418	0.016	Benign	No
66	P4048L	CCG>CTG	Somatic	0.480	0.125	0.188	0.455	0.039	Benign	No
67	L4222V	CTA>GTA	Somatic	0.548	0.228	0.268	0.344	0.967	Probably damaging	No
83	R2922W	CGG>TGG	Somatic	0.302	0.012	0.609	0.119	0.928	Probably damaging	No
87	N5222K	AAC>AAA	Somatic	0.704	0.616	0.235	0.386	0.446	Benign	FYR-N
U100	F2536S	TTC>TCC	Somatic	0.530	0.196	0.76	0.059	0.535	Possibly damaging	No

[a]N.d. = not determined due to absent normal tissue.
[b]CHASM = Cancer-specific High-throughput Annotation of Somatic Mutations, driver score interpretation: true driver mutations close to 0, functional score: close to 1 means functional effect.
[c]PolyPhen2 = Polymorphism Phenotyping v2, non-synonomous missense variant prediction.

p.H154Y mutation in *calmodulin binding transcription activator 1* (*CAMTA1*), a gene located on chromosome 1p36, a frequently deleted region in adrenomedullary tumors (Edström Elder et al., 2002; Fig. 1A). Moreover, Case 34 displaying a constitutional *RET* gene mutation exhibits an equivocal pathology report suggestive of malignant features, but not fulfilling histological criteria for malignancy. As a very low malignancy rate is reported for PCCs in MEN2a patients, we included this case as a part of the discovery cohort to detect eventual additional somatic driver gene mutations of interest. Indeed, in Case 34, we observed a somatic p.D76G mutation in the *cyclin-dependent kinase inhibitor 2C* (*CDKN2C*, *p18*), a gene previously showed to be mutated in human RET-associated PCCs (van Veelen et al., 2009; Fig. 1A, Supporting Information Table 3).

Mutational Gene Ontology Analysis

Gene ontology analyses were performed using The Database for Annotation, Visualization and Integrated Discovery (DAVID) database. These analyses identified an enrichment of somatic mutations in apoptosis-related pathways, as nonsynonymous mutations in 10 different genes annotated as "apoptosis-related" were seen (*ANXA1*, *BIRC6*, *CD5*, *CDKN2C*, *HMOX1*, *HRAS*, *MITF*, *NOX5*, *NTF3*, and *RYR2*). This finding constituted the top enriched biological process, as these genes constitute approximately 10% of all mutated genes in the discovery cohort. Other significant gene ontology enrichments comprised chordate embryonic development (seven mutated genes; *EPAS1*, *KMT2D/MLL2*, *PROX1*, *RIC8A*, *SFRP2*, *TSC2*, *WDTC1*) and chemotaxis (four mutated genes; *CXCL13*, *HRAS*, *PLD1*, *TSC2*).

Custom Amplicon *KMT2D* Sequencing

A verification cohort of 83 additional PCCs was collected and analyzed for *KMT2D* gene mutations by focused sequencing of exomic regions and exon–intron boundaries using molecular inversion probes (Supporting Information Table 1). This lead to the discovery of 11 additional heterozygous missense variants in 83 PCCs (13%), all verified using Sanger sequencing. Ten of the *KMT2D* variants detected in PCCs were verified somatic based on the finding of wild-type sequences in DNA from constitutional tissues, whereas two variants were found also in

constitutional tissues and one was termed undetermined due to the lack of normal tissues (Table 1, Supporting Information Fig. 1, Supporting Information Table 3). In total, heterozygous missense *KMT2D* variants were found in 14 out of 99 PCCs sequenced (14%; 13 of 89 Swedish cases, 1 of 10 US cases), and two recurrent variants (p.G2735S and p.N5223S) were seen in two independent PCCs, respectively.

In Silico Mutation Prediction Analyses

To assess the pathogenic nature of the *KMT2D* mutations discovered in our cohorts, we assessed the individual variants using a bioinformatical screening process incorporating the established mutation prediction softwares cancer-specific high-throughput annotation of somatic mutations (CHASM) and PolyPhen 2 HumDiv (Carter et al., 2009; Adzhubei et al., 2010). The results indicate that subsets of the detected *KMT2D* mutations are predicted to be of functional significance as supported by these independent prediction softwares (Table 1). Moreover, a schematic overview of significant KMT2D binding partners was obtained through the Search Tool for the Retrieval of Interacting Genes/Proteins (String) database (Fig. 2B).

Constitutional *KMT2D* Variants

Two constitutional variants (p.G2735S in Case 6 and p.Q1023K in Case 27) were observed. Case 6 is 44-year-old female with a benign PCC without signs of recurrent disease, also displaying history of an invasive ductal carcinoma of the breast. Case 27 is a 52-year-old female with a benign PCC, no recurrences and no additional tumors. Both patients lack positive family history indicative of tumor susceptibility syndromes, and no indications of Kabuki syndrome-related features were found. No parental samples were available for further genetic characterization. The same screening was carried out for a third patient (Case 3) with a *KMT2D* variant that could not be verified as somatic or constitutional due to lack of normal tissue.

Comparison to Established Genotypes and Clinical Parameters

Using the previously established genotypes in the Swedish PCC subset of the verification cohort ($n = 73$), a detailed mapping of case-by-case mutational burden regarding the 10 out of the 13 susceptibility genes that were found mutated in any of the PCCs (including *KMT2D*) was performed (Welander et al., 2012, 2014b; Fig. 1B). *KMT2D* was found mutated in 13 Swedish PCC cases, constituting 25% of the PCCs with any known susceptibility gene mutation (Fig. 1B). Seven of the 13 PCCs with *KMT2D* mutations did not display mutations in other PCC susceptibility genes (54%), whereas the remaining six cases also carried mutations in either *NF1* (three cases), *RET* (two cases), or *TMEM127* (one case) (Fig. 1B).

Tumors with *KMT2D* mutations were found to be significantly larger than tumors with other known PCC susceptibility gene mutations (Two-tailed Mann–Whitney *U* test, $P = 0.039$, Fig. 3A). Full biochemical data was available for 11 PCCs with *KMT2D* mutations, 10 of which displayed increased serum norepinephrine levels (Supporting Information Table 1). Although not statistically significant, this trend may indicate an underlying biochemical correlation between *KMT2D* mutations and serum norepinephrine. *KMT2D* mutations were not significantly associated with gender, age, or malignancy status (Supporting Information Table 1).

KMT2D Expressional and Copy Number Analyses

The copy number of *KMT2D* was determined in 86 PCCs using a TaqMan Copy Number Assay targeting the *KMT2D* locus. While the vast majority of samples ($n = 78$; 91%) were diploid for *KMT2D*, a small subset did exhibit one ($n = 2$; 2%), three ($n = 5$; 6%), or four ($n = 1$; 1%) copies (Supporting Information Table 4). All *KMT2D*-mutated cases available for copy number analyses were diploid for the *KMT2D* locus, and hence mutations and copy number alterations were mutually exclusive.

KMT2D expressional analyses using quantitative RT-PCR (qRT-PCR) were undertaken for PCCs for which RNA was available ($n = 69$) and for normal adrenal samples ($n = 10$) as well as normal adrenal medulla ($n = 1$). The *KMT2D* gene was found expressed in all PCCs tested, with a relative expression compared to normal adrenal mean ranging from 0.429 to 6.257 and the normal adrenomedullary biopsy exhibited *KMT2D* levels on par with the 10 normal whole-adrenals used as normalization controls (Fig. 3B, Supporting Information Table 4). Furthermore, *KMT2D* expression was significantly increased in PCCs compared to normal adrenals (Two-tailed Mann–Whitney *U* test, $P = 0.017$) but did not significantly differ between *KMT2D*-mutated and wild-type cases.

KMT2D immunohistochemistry was performed for all cases with available formalin-fixated and

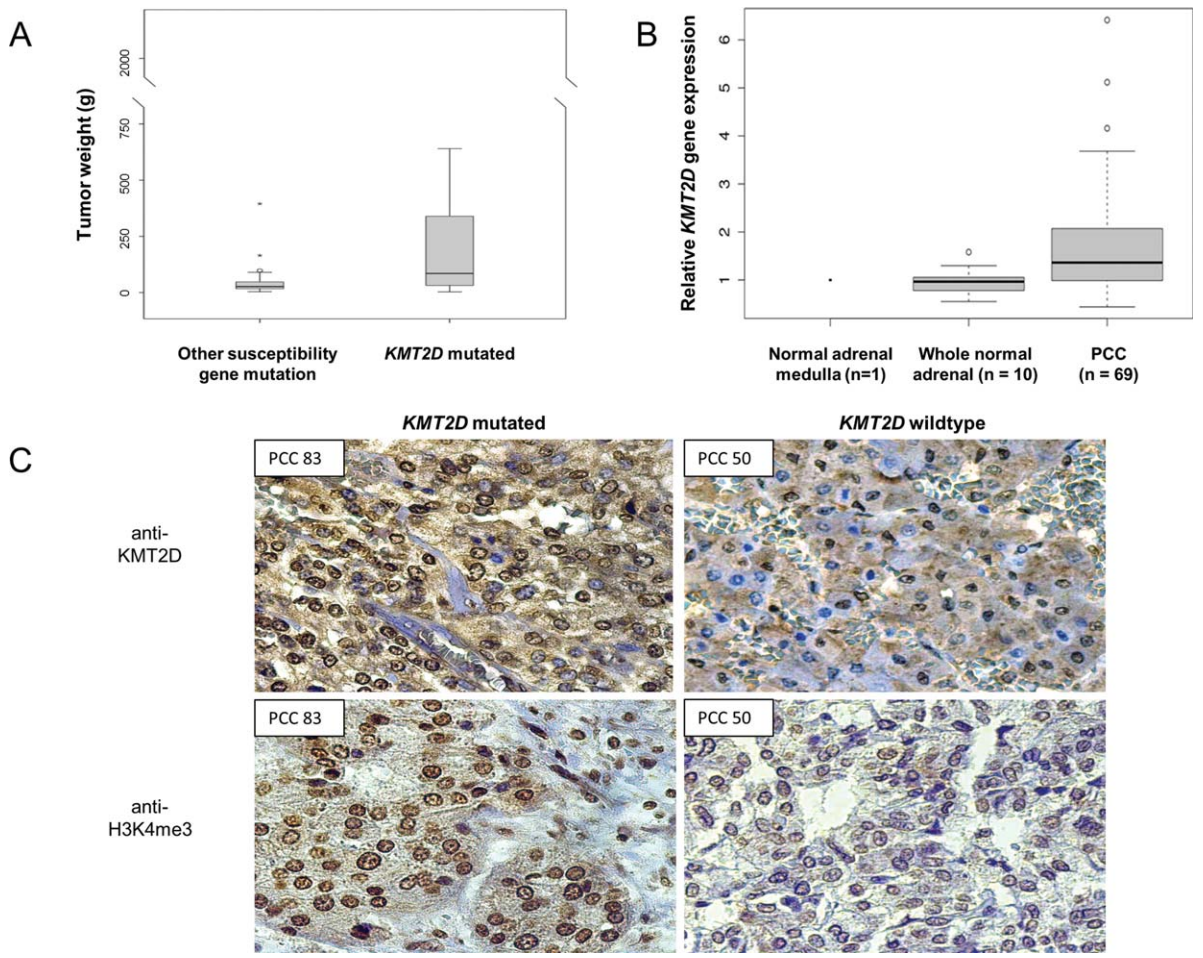

Figure 3. *KMT2D* expressional analyses and mutational correlation to PCC tumor weight. (A) PCCs with *KMT2D* mutations display significantly larger tumor weight as compared to PCCs with mutations in other susceptibility genes (Two-tailed Mann–Whitney *U* test, $P = 0.039$). (B) Box plot depicting *KMT2D* mRNA expression in one normal adrenal medulla biopsy (left), 10 whole normal adrenal samples (middle) versus 69 PCCs (right) with relative expression to the whole normal adrenal mean on the *Y* axis. PCCs had significantly higher relative *KMT2D* expression than normal adrenal glands (Two-tailed Mann–Whitney *U* test, $P = 0.017$). (C) Examples of immunohistochemical stainings using anti-KMT2D and anti-H3K4me3 antibodies in the *KMT2D*-mutated PCC 83 (left) with positive nuclear staining (>75% of tumor nuclei stained) compared to the *KMT2D* wild-type PCC 50 (right) with partially positive staining patterns (50–75% tumor nuclei stained). All cases stained for KMT2D additionally displayed low to moderate levels of cytoplasmic immunoreactivity. [Color figure can be viewed in the online issue, which is available at wileyonlinelibrary.com.]

paraffin-embedded (FFPE) tissues ($n = 65$). All PCCs either stained positive (>75% positive tumor nuclei, $n = 28$) or partially positive (50–75% positive tumor nuclei, $n = 37$) for nuclear KMT2D (Fig. 3C, Supporting Information Table 4). Statistically, *KMT2D*-mutatedcases more frequently displayed positive KMT2D nuclear staining than wild-type cases (Fisher's exact, $P = 0.032$). Moreover, 19 tumors (10 *KMT2D* wild-type and 9 with somatic *KMT2D* mutations) were furthermore assessed for immunohistochemistry using an anti-H3K4me3 antibody, as KMT2D conveys trimethylation of histone-3 lysine-4 (Kim et al., 2014). Thirteen PCCs (of which 6 *KMT2D* mutated) displayed positive nuclear staining and the remaining six (including 3 *KMT2D* mutated) exhibited partially positive immunoreactivity (Fig. 3C, Supporting Information Table 4). A significant correlation between cases with positive KMT2D nuclear staining and cases with positive H3K4me3 nuclear staining was observed (Fisher's exact, $P = 0.038$).

A subset of PCCs ($n = 18$; eight *KMT2D* mutated and 10 *KMT2D* wild type) was assessed for H3K27me3, as activation of gene expression in the related tumor-type medulloblastoma is concerted through increased H3K4me3 and reduction of H3K27me3 levels, respectively (Dubuc et al., 2013). Sixteen cases either stained negative ($n = 6$) or mixed, displaying nuclear H3K27me3 immunoreactivity in 25–75% of tumor cells ($n = 10$). Interestingly, all six H3K27me3 negative cases exhibited strong H3K4me3 staining, and

four of them displayed somatic *KMT2D* mutations. 11 out of the 13 H3K4me3-positive PCCs (85%) exhibited either negative or mixed H3K27me3, only two were H3K27me3 positive. These results suggest that the majority of H3K4me3-positive cases seem to exhibit reduced levels of H3K27me3, and that H3K27me3-negative PCCs are associated to strong H3K4me3 levels as well as *KMT2D* mutations (Supporting Information Table 4).

SDHB Expressional Analyses

All PCCs ($n = 16$) in the discovery cohort and 73 of the 83 PCCs included in the verification cohort have been previously screened for PCC susceptibility gene mutations, (including *SDHB*), however, no *SDHB* mutations were found among the 89 PCCs tested (Supporting Information Table 1). To test whether *KMT2D* mutations could potentially affect the SDHB expressional status, we gathered available FFPE tissue from 14 PCCs (including five cases with *KMT2D* mutations) and 13 paragangliomas. The paragangliomas were included as negative and positive controls. SDHB immunohistochemistry was performed using a standardized protocol as detailed in the Supporting Information Materials and Methods section. All PCCs analyzed, except two cases endowed with *SDHA* mutations, displayed strong cytoplasmic SDHB immunoreactivity (Supporting Information Table 4). This is in line with the wild-type *SDHB* status for these cases. Also, the retained SDHB expression found in *KMT2D*-mutated PCCs suggest that SDHB expression is not disrupted through *KMT2D* mutations. Five of the 13 paragangliomas displayed *SDHB* mutations, and all *SDHB*-mutated cases displayed negative SDHB expression as expected, serving as negative controls for the experiments (data not shown).

Functional *KMT2D* Experiments

The functional outcome of *KMT2D* siRNA knockdown and *KMT2D* constitutive overexpression in the rat PCC cell line PC12-Adh was analyzed. While no significant effect on viability or loss of viability was seen upon *KMT2D* siRNA knockdown (Supporting Information Fig. 2), *KMT2D* silencing significantly reduced the motility of PC12-Adh cells (Fig. 4). A significant increase in cellular motility was similarly observed when constitutively overexpressing *KMT2D* in the same cell line, and the findings were furthermore supported by transient overexpression analyses (Fig. 4).

Expressional Profiling Of *KMT2D* Overexpressed PC12 Cells

The RNA expressional profile of PC12 cells with and without *KMT2D* overexpression was studied using a high-resolution Affymetrix array technique as described in detail in the Supporting Information Materials and Methods section. A significant difference in expressional patterns between mock-transfected and *KMT2D*-transfected PC12 cells was found for a total of 594 transcripts ($P = 0.01$; Supporting Information Table 5). Gene ontology analyses were undertaken using the KEGG pathway analysis at the DAVID database suggesting significant enrichment of genes within the Transforming growth factor beta (TGF-beta) signaling network and extracellular matrix–receptor interaction pathways ($P = 6.7 \times 10^{-12}$ and 1.1×10^{-10}, respectively). Furthermore, in descending order of significance, the DAVID database suggests regulation of the following top five pathways when comparing PC12 cells with and without *KMT2D* overexpression (all with significant associations $P < 5.3 \times 10^{-8}$): axon guidance, regulation of actin cytoskeleton, focal adhesion, and pathways in cancer. The finding of axon guidance and TGF-beta signaling pathways as significantly altered molecular networks in *KMT2D*-transfected PC12 cells compared to mock controls was furthermore supported by supplementary gene ontology analyses in which only transcripts with absolute fold changes of 1.5 or above were considered biologically relevant and included in the analysis (data not shown). Moreover, as detailed in Supporting Information Table 5, *CDH2* and *ITGBL1* (*Cadherin-2* and *Integrin beta-like 1* respectively) were two of the most down regulated genes.

DISCUSSION

In this study, WES was performed for a well-characterized PCC cohort devoid of established constitutional susceptibility gene mutations, identifying several interesting alterations, including the novel recognition of *KMT2D* and *ZAN* as recurrently mutated COSMIC genes. Furthermore, nonrecurrent mutations in the cancer-associated genes *MITF*, *WDTC1*, *CAMTA1*, and *CDKN2C* were detected in cases lacking other credible somatic driver events. Overall, somatic mutations

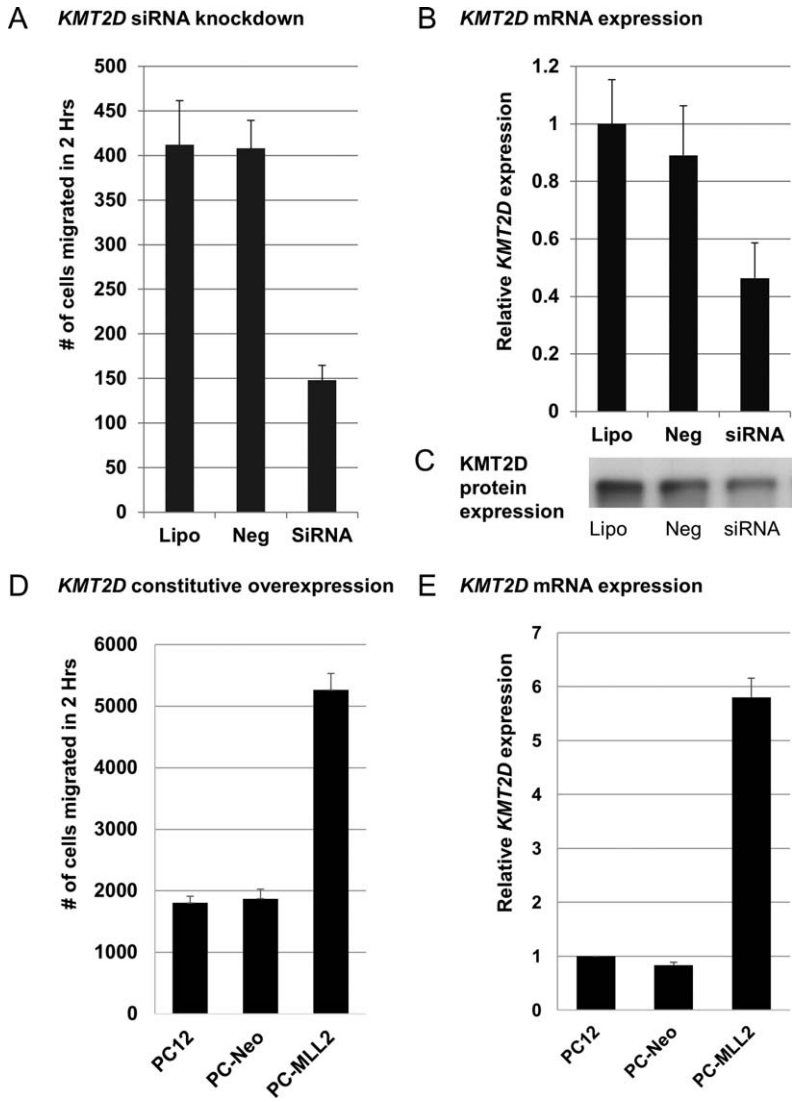

Figure 4. *KMT2D* affects the migratory potential of PC12-Adh cells. (A) PC12-Adh cells were treated with Lipofectamine 2000 (denoted Lipo), scrambled siRNA (denoted Neg), or specific siRNA (denoted siRNA) against *KMT2D* for 48 hr, trypsinized and allowed to migrate through a modified Boyden chamber for 2 hr, fixed, stained and the migrated cells were counted. Downregulation of *KMT2D* mRNA (B) and protein (C) were determined by qRT-PCR and Western blotting, respectively. (D) Constitutive *KMT2D* expression in PC12-Adh cells leads to an increase in migration through a modified Boyden chamber counted after 2 hr. PC12: untransfected control, PC-Neo: mock-transfected clone, and PC-MLL2: *KMT2D*-transfected clone. Upregulation of *KMT2D* mRNA was demonstrated by qRT-PCR (E).

aggregated in apoptotic-related pathways, which might indicate that aberrancies in signaling pathways controlling programmed cell death partly account for the development of PCCs.

Although adrenomedullary tumors have been previously investigated using next-generation sequencing, this is to our knowledge the first study that specifically targets a cohort enriched for genetic orphan PCCs to detect novel genes implicated in PCC development. We hypothesized that residual, nonestablished genetic events in PCCs potentially detectable through WES would probably occur at low frequencies. To ensure an adequate sensitivity for detecting these remaining causal variants, a large number of PCCs would be needed. Given the well-known rarity of adrenomedullary tumors, we selectively chose PCCs devoid of known PCC susceptibility gene mutations (somatic and constitutional) to counter this issue.

KMT2D was identified as the most recurrently mutated cancer gene in our discovery cohort, and extended investigations in a validation cohort revealed missense variants in 14% of the PCCs studied. Expressional *KMT2D* analyses indicate overexpression in PCCs compared to normal

tissues, and nuclear KMT2D expression was significantly associated to trimethylation of H3K4. The protein encoded by *KMT2D* is a histone methyltransferase that regulates DNA accessibility (Kim et al., 2014). Germline mutations in this gene have been shown to be a cause of Kabuki syndrome (OMIM #147920), a developmental disorder characterized by postnatal dwarfism, specific facial features as well as intellectual disability (Ng et al., 2010; Li et al., 2011; Paulussen et al., 2011). *KMT2D* is recurrently mutated in non-Hodgkin lymphoma (Morin et al., 2011; Okosun et al., 2014), and mutations have also been reported in epithelial tumors such as medulloblastoma, urinary bladder carcinoma, esophageal squamous cell carcinoma, and small cell lung cancer (Parsons et al., 2011; Balbás-Martínez et al., 2013; Dubuc et al., 2013; Lin et al., 2014; Ross et al., 2014; Song et al., 2014). Knockdown of *KMT2D* causes dysregulation of adhesion-related cytoskeletal events in vitro that in turn affect cell growth and survival, and *KMT2D* has been shown to exhibit tumor suppressor as well as oncogenic properties for various tumors (Issaeva et al., 2007; Natarajan et al., 2010; Guo et al., 2013; Kim et al., 2014). In this study, PCCs with *KMT2D* mutations were found to be significantly larger than tumors with other known PCC susceptibility gene mutations, suggesting that *KMT2D* mutations might positively influence tumor growth in PCCs. Indeed, the observed effects on cell motility upon *KMT2D* overexpression suggest that *KMT2D* potentially might harbor oncogenic properties in PCCs, and we, therefore, speculate that the *KMT2D* mutations observed here could be activating rather than deleterious. Interestingly, *KMT2D*-transfected PC12 cells were shown to exhibit a transcriptional profile enriched for genes within the TGF-beta signaling network and extracellular matrix–receptor interaction pathways, as well as for genes involved in the regulation of actin cytoskeleton and focal adhesion. This analysis could possibly explain why *KMT2D* transfected PC12 cells exhibited an increased migratory potential, since the TGF-beta pathway as well as the triad extracellular matrix, focal adhesion and regulation of actin cytoskeleton are important players in mediating migratory potential and invasive properties of various tumor types. Moreover, as *CDH2* and *ITGBL1* (*Cadherin-2* and *Integrin beta-like 1*, respectively) were two of the most downregulated genes, this might suggest a potential role for *KMT2D* regulation of cadherins and integrins in mediating the migratory phenotype of PC12 cells.

In cancer genetics, recurrent somatic variants usually indicate specific underlying mechanisms that in turn may highlight disease-related properties for a specific gene, as identical variants are not expected to occur independently by random chance. In our study, the recurrent *KMT2D* variants p.G2735S and p.N5223S were seen in two independent PCCs, respectively. Interestingly, in addition to the p.N5223S mutations, a p.N5222K somatic mutation was also detected in an independent PCC sample, furthermore pinpointing the FYR-N domain of *KMT2D* as a region of potential importance in PCCs. A FYR domain is regularly found in chromatin-associated proteins, containing sequence motifs rich in phenylalanine/tyrosine residues of unknown function, and the aggregation of somatic mutations observed in this study would suggest that this region may be linked functionally to the development of a small subset of PCCs. Overall, five PCCs displayed somatic mutations in the functional FYR or SET domains of KMT2D (Table 1), constituting 36% of all *KMT2D*-mutated PCCs in this study (Fig. 2A). Moreover, the finding of strong nuclear H3K4me3 levels in cases with *KMT2D* mutations vaguely suggests that the mutations affect the histone methyltransferase activity of KMT2D. However, as a significant proportion of the *KMT2D* mutations detected were not located within KMT2D domains with established methyltransferase-associated functions, it is possible that a subset of these mutations exert their function through disruption/increased affinity of important *KMT2D* binding partners, such as *ESR1*, *KDM6A*, and *WDR5* to name a few (Fig. 2B). Notably, in silico analyses did not support a pathogenic role for a subset of the observed mutations, characterized by low PolyPhen2 or CHASM functional scores. Together with the fact that KMT2D expression did not significantly differ between *KMT2D*-mutated and wild-type cases, this could imply that subsets of the observed *KMT2D* mutations in fact are passenger events occurring randomly. As the size of *KMT2D* prevented a site-directed mutagenesis approach to study the functional consequences of the missense variants, the true pathogenic nature of the *KMT2D* somatic mutations discovered in this study remains to be established. Future studies will possibly elucidate whether *KMT2D* should be regarded as an oncogene or tumor suppressor in adrenomedullary tumors.

Both patients (cases 3 and 27) exhibiting PCC and constitutional *KMT2D* variants lacked positive family history for either Kabuki syndrome as well as adrenomedullary disease. Also, the mutation prediction analyses did not point out the two

constitutional variants to be of pathogenic significance, and hence the importance of these findings remains unclear. Even so, cases 3 and 6 both exhibited the recurrent p.G2735S variant, and both cases displayed ductal carcinoma in situ and invasive ductal carcinoma of the breast, respectively. Although Case 3 was not available for constitutional testing, the co-occurrence of PCC and malignant breast tumors in these two unrelated cases with an identical *KMT2D* variant is intriguing, and might suggest an underlying tumor phenotype.

To conclude, *KMT2D* is a recurrently mutated gene in PCCs. As more than half of the *KMT2D*-mutated tumors lack mutations in other known PCC susceptibility genes, *KMT2D* mutations could denote a novel genetic mechanism with possible implications for PCC tumorigenesis. The observation that *KMT2D* regulates adrenomedullary cell migration indicates that dysregulation of this intriguing methyltransferase might constitute a potential novel pathogenic mechanism for subsets of PCCs.

ACKNOWLEDGMENTS

The authors are indebted to Dr. Catharina Larsson, Karolinska Institutet, Stockholm, Sweden for scientific communications and to Annette Molbaek, Linköping University, Linköping, Sweden for performing RNA microarray analysis.

REFERENCES

Adzhubei IA, Schmidt S, Peshkin L, Ramensky VE, Gerasimova A, Bork P, Kondrashov AS, Sunyaev SR. 2010. A method and server for predicting damaging missense mutations. Nat Methods 7: 248–9.

Alhopuro P, Sammalkorpi H, Niittymäki I, Biström M, Raitila A, Saharinen J, Nousiainen K, Lehtonen HJ, Heliövaara E, Puhakka J, Tuupanen S, Sousa S, Seruca R, Ferreira AM, Hofstra RM, Mecklin JP, Järvinen H, Ristimäki A, Orntoft TF, Hautaniemi S, Arango D, Karhu A, Aaltonen LA. 2012. Candidate driver genes in microsatellite-unstable colorectal cancer. Int J Cancer 130: 1558–66.

Balbás-Martínez C, Sagrera A, Carrillo-de-Santa-Pau E, Earl J, Márquez M, Vazquez M, Lapi E, Castro-Giner F, Beltran S, Bayés M, Carrato A, Cigudosa JC, Domínguez O, Gut M, Herranz J, Juanpere N, Kogevinas M, Langa X, López-Knowles E, Lorente JA, Lloreta J, Pisano DG, Richart L, Rico D, Salgado RN, Tardón A, Chanock S, Heath S, Valencia A, Losada A, Gut I, Malats N, Real FX. 2013. Recurrent inactivation of STAG2 in bladder cancer is not associated with aneuploidy. Nat Genet 45:1464–9.

Brito JP, Asi N, Bancos I, Gionfriddo MR, Zeballos-Palacios CL, Leppin AL, Undavalli C, Wang Z, Domecq JP, Prustsky G, Elraiyah TA, Prokop LJ, Montori VM, Murad MH. 2015. Testing for germline mutations in sporadic pheochromocytoma/paraganglioma: a systematic review. Clin Endocrinol 82:338–45.

Burnichon N, Buffet A, Parfait B, Letouzé E, Laurendeau I, Loriot C, Pasmant E, Abermil N, Valeyrie-Allanore L, Bertherat J, Amar L, Vidaud D, Favier J, Gimenez-Roqueplo AP. 2012. Somatic NF1 inactivation is a frequent event in sporadic pheochromocytoma. Hum Mol Genet 21:5397–405.

Carter H, Chen S, Isik L, Tyekucheva S, Velculescu VE, Kinzler KW, Vogelstein B, Karchin R. 2009. Cancer-specific high-throughput annotation of somatic mutations: computational prediction of driver missense mutations. Cancer Res 69:6660–7.

Castro-Vega LJ, Buffet A, De Cubas AA, Cascón A, Menara M, Khalifa E, Amar L, Azriel S, Bourdeau I, Chabre O, Currás-Freixes M, Franco-Vidal V, Guillaud-Bataille M, Simian C, Morin A, Letón R, Gómez-Graña A, Pollard PJ, Rustin P, Robledo M, Favier J, Gimenez-Roqueplo AP. 2014. Germline mutations in FH confer predisposition to malignant pheochromocytomas and paragangliomas. Hum Mol Genet 23:2440–6.

Comino-Méndez I, Gracia-Aznárez FJ, Schiavi F, Landa I, Leandro-García LJ, Letón R, Honrado E, Ramos-Medina R, Caronia D, Pita G, Gómez-Graña A, de Cubas AA, Inglada-Pérez L, Maliszewska A, Taschin E, Bobisse S, Pica G, Loli P, Hernández-Lavado R, Díaz JA, Gómez-Morales M, González-Neira A, Roncador G, Rodríguez-Antona C, Benítez J, Mannelli M, Opocher G, Robledo M, Cascón A. 2011. Exome sequencing identifies MAX mutations as a cause of hereditary pheochromocytoma. Nat Genet 43:663–7.

Comino-Méndez I, de Cubas AA, Bernal C, Álvarez-Escolá C, Sánchez-Malo C, Ramírez-Tortosa CL, Pedrinaci S, Rapizzi E, Ercolino T, Bernini G, Bacca A, Letón R, Pita G, Alonso MR, Leandro-García LJ, Gómez-Graña A, Inglada-Pérez L, Mancikova V, Rodríguez-Antona C, Mannelli M, Robledo M, Cascón A. 2013. Tumoral EPAS1 (HIF2A) mutations explain sporadic pheochromocytoma and paraganglioma in the absence of erythrocytosis. Hum Mol Genet 22:2169–76.

Crona J, Delgado Verdugo A, Maharjan R, Stålberg P, Granberg D, Hellman P, Björklund P. 2013. Somatic mutations in H-RAS in sporadic pheochromocytoma and paraganglioma identified by exome sequencing. J Clin Endocrinol Metab 98:E1266–71.

Cronin JC, Wunderlich J, Loftus SK, Prickett TD, Wei X, Ridd K, Vemula S, Burrell AS, Agrawal NS, Lin JC, Banister CE, Buckhaults P, Rosenberg SA, Bastian BC, Pavan WJ, Samuels Y. 2009. Frequent mutations in the MITF pathway in melanoma. Pigment Cell Melanoma Res 22:435–44.

Crossey PA, Richards FM, Foster K, Green JS, Prowse A, Latif F, Lerman MI, Zbar B, Affara NA, Ferguson-Smith MA, Maher ER. 1994. Identification of intragenic mutations in the von Hippel-Lindau disease tumour suppressor gene and correlation with disease phenotype. Hum Mol Genet 3:1303–8.

Dahia PLM. 2014. Pheochromocytoma and paraganglioma pathogenesis: learning from genetic heterogeneity. Nat Rev Cancer 14:108–19.

DeLellis RA, Lloyd RV, Heitz PU, Eng C. 2004. World Health Organization Classification of Tumours. Pathology and Genetics of Tumours of Endocrine Organs. Lyon: IARC Press. p 147–166.

Dubuc AM, Remke M, Korshunov A, Northcott PA, Zhan SH, Mendez-Lago M, Kool M, Jones DT, Unterberger A, Morrissy AS, Shih D, Peacock J, Ramaswamy V, Rolider A, Wang X, Witt H, Hielscher T, Hawkins C, Vibhakar R, Croul S, Rutka JT, Weiss WA, Jones SJ, Eberhart CG, Marra MA, Pfister SM, Taylor MD. 2013. Aberrant patterns of H3K4 and H3K27 histone lysine methylation occur across subgroups in medulloblastoma. Acta Neuropathol 125:373–84.

Edström Elder E, Nord B, Carling T, Juhlin C, Bäckdahl M, Höög A, Larsson C. 2002. Loss of heterozygosity on the short arm of chromosome 1 in pheochromocytoma and abdominal paraganglioma. World J Surg 26:965–71.

Eisenhofer G, Huynh T-T, Pacak K, Brouwers FM, Walther MM, Linehan WM, Munson PJ, Mannelli M, Goldstein DS, Elkahloun AG. 2004. Distinct gene expression profiles in norepinephrine- and epinephrine-producing hereditary and sporadic pheochromocytomas: activation of hypoxia-driven angiogenic pathways in von Hippel-Lindau syndrome. Endocr Relat Cancer 11:897–911.

Favier J, Amar L, Gimenez-Roqueplo A-P. 2015. Paraganglioma and phaeochromocytoma: from genetics to personalized medicine. Nat Rev Endocrinol 11:101–11.

Guo C1, Chen LH, Huang Y, Chang CC, Wang P, Pirozzi CJ, Qin X, Bao X, Greer PK, McLendon RE, Yan H, Keir ST, Bigner DD, He Y. 2013. KMT2D maintains neoplastic cell proliferation and global histone H3 lysine 4 monomethylation. Oncotarget 4:2144–53.

Issaeva I, Zonis Y, Rozovskaia T, Orlovsky K, Croce CM, Nakamura T, Mazo A, Eisenbach L, Canaani E. 2007. Knockdown of ALR (MLL2) reveals ALR target genes and leads to alterations in cell adhesion and growth. Mol Cell Biol 27:1889–903.

Kim J-H, Sharma A, Dhar SS, Lee S-H, Gu B, Chan C-H, Lin H-K, Lee MG. 2014. UTX and MLL4 coordinately regulate

transcriptional programs for cell proliferation and invasiveness in breast cancer cells. Cancer Res 74:1705–17.

Lack EE. 2007. American Registry of Pathology, and Armed Forces Institute of Pathology. Tumors of the adrenal glands and extraadrenal paraganglia. Washington DC: American Registry of Pathology in collaboration with the Armed Forces Institute of Pathology. p: 274–276.

Ladroue C, Carcenac R, Leporrier M, Gad S, Le Hello C, Galateau-Salle F, Feunteun J, Pouysségur J, Richard S, Gardie B. 2008. PHD2 mutation and congenital erythrocytosis with paraganglioma. N Engl J Med 359:2685–92.

Li Y, Bögershausen N, Alanay Y, Simsek Kiper PO, Plume N, Keupp K, Pohl E, Pawlik B, Rachwalski M, Milz E, Thoenes M, Albrecht B, Prott EC, Lehmkühler M, Demuth S, Utine GE, Boduroglu K, Frankenbusch K, Borck G, Gillessen-Kaesbach G, Yigit G, Wieczorek D, Wollnik B. 2011. A mutation screen in patients with Kabuki syndrome. Hum Genet 130: 715–24.

Lin DC, Hao JJ, Nagata Y, Xu L, Shang L, Meng X, Sato Y, Okuno Y, Varela AM, Ding LW, Garg M, Liu LZ, Yang H, Yin D, Shi ZZ, Jiang YY, Gu WY, Gong T, Zhang Y, Xu X, Kalid O, Shacham S, Ogawa S, Wang MR, Koeffler HP. 2014. Genomic and molecular characterization of esophageal squamous cell carcinoma. Nat Genet 46:467–73.

Morin RD, Mendez-Lago M, Mungall AJ, Goya R, Mungall KL, Corbett RD, Johnson NA, Severson TM, Chiu R, Field M, Jackman S, Krzywinski M, Scott DW, Trinh DL, Tamura-Wells J, Li S, Firme MR, Rogic S, Griffith M, Chan S, Yakovenko O, Meyer IM, Zhao EY, Smailus D, Moksa M, Chittaranjan S, Rimsza L, Brooks-Wilson A, Spinelli JJ, Ben-Neriah S, Meissner B, Woolcock B, Boyle M, McDonald H, Tam A, Zhao Y, Delaney A, Zeng T, Tse K, Butterfield Y, Birol I, Holt R, Schein J, Horsman DE, Moore R, Jones SJ, Connors JM, Hirst M, Gascoyne RD, Marra MA. 2011. Frequent mutation of histone-modifying genes in non-Hodgkin lymphoma. Nature 476:298–303.

Natarajan TG, Kallakury BV, Sheehan CE, Bartlett MB, Ganesan N, Preet A, Ross JS, Fitzgerald KT. 2010. Epigenetic regulator MLL2 shows altered expression in cancer cell lines and tumors from human breast and colon. Cancer Cell Int 10:13.

Ng SB, Bigham AW, Buckingham KJ, Hannibal MC, McMillin MJ, Gildersleeve HI, Beck AE, Tabor HK, Cooper GM, Mefford HC, Lee C, Turner EH, Smith JD, Rieder MJ, Yoshiura K, Matsumoto N, Ohta T, Niikawa N, Nickerson DA, Bamshad MJ, Shendure J. 2010. Exome sequencing identifies MLL2 mutations as a cause of Kabuki syndrome. Nat Genet 42:790–3.

Okosun J, Bödör C, Wang J, Araf S, Yang CY, Pan C, Boller S, Cittaro D, Bozek M, Iqbal S, Matthews J, Wrench D, Marzec J, Tawana K, Popov N, O'Riain C, O'Shea D, Carlotti E, Davies A, Lawrie CH, Matolcsy A, Calaminici M, Norton A, Byers RJ, Mein C, Stupka E, Lister TA, Lenz G, Montoto S, Gribben JG, Fan Y, Grosschedl R, Chelala C, Fitzgibbon J. 2014. Integrated genomic analysis identifies recurrent mutations and evolution patterns driving the initiation and progression of follicular lymphoma. Nat Genet 46:176–81.

Parsons DW, Li M, Zhang X, Jones S, Leary RJ, Lin JC, Boca SM, Carter H, Samayoa J, Bettegowda C, Gallia GL, Jallo GI, Binder ZA, Nikolsky Y, Hartigan J, Smith DR, Gerhard DS, Fults DW, VandenBerg S, Berger MS, Marie SK, Shinjo SM, Clara C, Phillips PC, Minturn JE, Biegel JA, Judkins AR, Resnick AC, Storm PB, Curran T, He Y, Rasheed BA, Friedman HS, Keir ST, McLendon R, Northcott PA, Taylor MD, Burger PC, Riggins GJ, Karchin R, Parmigiani G, Bigner DD, Yan H, Papadopoulos N, Vogelstein B, Kinzler KW, Velculescu VE. 2011. The genetic landscape of the childhood cancer medulloblastoma. Science 331:435–9.

Paulussen AD, Stegmann AP, Blok MJ, Tserpelis D, Posma-Velter C, Detisch Y, Smeets EE, Wagemans A, Schrander JJ, van den Boogaard MJ, van der Smagt J, van Haeringen A, Stolte-Dijkstra I, Kerstjens-Frederikse WS, Mancini GM, Wessels MW, Hennekam RC, Vreeburg M, Geraedts J, de Ravel T, Fryns JP, Smeets HJ, Devriendt K, Schrander-Stumpel CT. 2011. MLL2 mutation spectrum in 45 patients with Kabuki syndrome. Hum Mutat 32:E2018–25.

Qin Y, Yao L, King EE, Buddavarapu K, Lenci RE, Chocron ES, Lechleiter JD, Sass M, Aronin N, Schiavi F, Boaretto F, Opocher G, Toledo RA, Toledo SP, Stiles C, Aguiar RC, Dahia PL. 2010. Germline mutations in TMEM127 confer susceptibility to pheochromocytoma. Nat Genet 42:229–33.

Ross JS, Wang K, Elkadi OR, Tarasen A, Foulke L, Sheehan CE, Otto GA, Palmer G, Yelensky R, Lipson D, Chmielecki J, Ali SM, Elvin J, Morosini D, Miller VA, Stephens PJ. 2014. Next-generation sequencing reveals frequent consistent genomic alterations in small cell undifferentiated lung cancer. J Clin Pathol 67:772–6.

Schlisio S, Kenchappa RS, Vredeveld LC, George RE, Stewart R, Greulich H, Shahriari K, Nguyen NV, Pigny P, Dahia PL, Pomeroy SL, Maris JM, Look AT, Meyerson M, Peeper DS, Carter BD, Kaelin WG Jr. 2008. The kinesin KIF1Bbeta acts downstream from EglN3 to induce apoptosis and is a potential 1p36 tumor suppressor. Genes Dev 22:884–93.

Song Y, Li L, Ou Y, Gao Z, Li E, Li X, Zhang W, Wang J, Xu L, Zhou Y, Ma X, Liu L, Zhao Z, Huang X, Fan J, Dong L, Chen G, Ma L, Yang J, Chen L, He M, Li M, Zhuang X, Huang K, Qiu K, Yin G, Guo G, Feng Q, Chen P, Wu Z, Wu J, Ma L, Zhao J, Luo L, Fu M, Xu B, Chen B, Li Y, Tong T, Wang M, Liu Z, Lin D, Zhang X, Yang H, Wang J, Zhan Q. 2014. Identification of genomic alterations in oesophageal squamous cell cancer. Nature 509:91–5.

van Veelen W, Klompmaker R, Gloerich M, van Gasteren CJ, Kalkhoven E, Berger R, Lips CJ, Medema RH, Höppener JW, Acton DS. 2009. P18 is a tumor suppressor gene involved in human medullary thyroid carcinoma and pheochromocytoma development. Int J Cancer 124:339–45.

Welander J, Soderkvist P, Gimm O. 2011. Genetics and clinical characteristics of hereditary pheochromocytomas and paragangliomas. Endocr Relat Cancer 18:R253–76.

Welander J, Larsson C, Bäckdahl M, Hareni N, Sivlér T, Brauckhoff M, Söderkvist P, Gimm O. 2012. Integrative genomics reveals frequent somatic NF1 mutations in sporadic pheochromocytomas. Hum Mol Genet 21:5406–16.

Welander J, Andreasson A, Brauckhoff M, Bäckdahl M, Larsson C, Gimm O, Söderkvist P. 2014a. Frequent EPAS1/HIF2α exons 9 and 12 mutations in non-familial pheochromocytoma. Endocr Relat Cancer 21:495–504.

Welander J, Andreasson A, Juhlin CC, Wiseman RW, Bäckdahl M, Höög A, Larsson C, Gimm O, Söderkvist P. 2014b. Rare germline mutations identified by targeted next-generation sequencing of susceptibility genes in pheochromocytoma and paraganglioma. J Clin Endocrinol Metab 99:E1352–60.

Zhuang Z, Yang C, Lorenzo F, Merino M, Fojo T, Kebebew E, Popovic V, Stratakis CA, Prchal JT, Pacak K. 2012. Somatic HIF2A gain-of-function mutations in paraganglioma with polycythemia. N Engl J Med 367:922–30.